Macromolecules

ARTICLE

pubs.acs.org/Macromolecules

Dependence of Thermal Stability on Molecular Structure of RAFT/MADIX Agents: A Kinetic and Mechanistic Study

Yanwu Zhou, Junpo He,* Changxi Li, Linxiang Hong, and Yuliang Yang

The State Key Laboratory of Molecular Engineering of Polymers, Department of Macromolecular Science, Fudan University, Shanghai 200433, China

Supporting Information

ABSTRACT: The thermal decomposition of different classes of RAFT/MADIX agents, namely dithioesters, trithiocarbonates, xanthates, and dithiocarbamates, were investigated through heating in solution. It was found that the decomposition behavior is complicated interplay of the effects of stabilizing Z-group and leaving R-group. The mechanism of the decomposition is mainly through three pathways, i.e., β-elimination, α-elimination, and homolysis of dithiocarbamate (particularly for universal RAFT agent). The most important pathway is the β-elimination of thiocarbonylthio compounds possessing β-hydrogen, leading to the formation unsaturated species. For the leaving group containing solely α-hydrogen, such as benzyl, α-elimination takes place, resulting in the formation of (*E*)-stilbene through a carbene intermediate. Homolysis occurs specifically in the case of a universal RAFT agent, in which a thiocarbonyl radical and an alkylthio radical are generated, finally forming thiolactone through a radical process. The stabilities of the RAFT/MADIX agents are investigated by measuring the apparent kinetics and activation energy of the thermal decomposition reactions. Both Z-group and R-group influence the stability of the agents through electronic and steric effects. Lone pair electron donating heteroatoms of Z-group show a remarkable stabilizing effect while electron withdrawing substituents, either in Z- or R-group, tends to destabilize the agent. In addition, bulkier or more β-hydrogens result in faster decomposition rate or lower decomposition temperature. Thus, the stability of the RAFT/MAIDX agents decreases in the order where R is (with identical Z = phenyl) $-CH_2Ph$ (**5**) > $-PS$ (PS-RAFT **15**) > $-C(Me)HPh$ (**2**) > $-C(Me)_2C(=O)OC_2H_5$ (**7**) > $-C(Me)_2Ph$(**1**) > $-PMMA$ (PMMA-RAFT **16**) > $-C(Me)_2CN$ (**6**). For those possessing identical leaving group such as 1-phenylethyl, the stability decreases in the order of *O*-ethyl (**11**) > $-N(CH_2CH_3)_2$ (**13**) > $-SCH(CH_3)Ph$ (**8**) > $-Ph$ (**2**) > $-CH_2Ph$ (**4**) > $-PhNO_2$ (**3**). These results consort with the chain transfer acitivities measured by the CSIRO group and agree well with the ab initio theoretical results by Coote. In addition, the difference between thermal stabilities of the universal RAFT agents at neutral and protonated states has also been demonstrated.

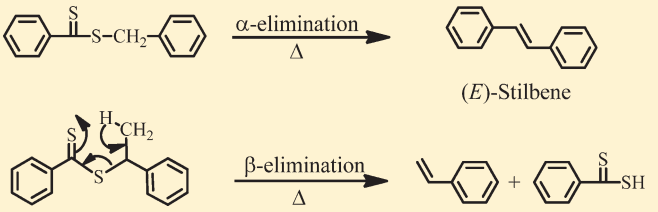

INTRODUCTION

Thiocarbonylthio compounds play the central role in reversible addition−fragmentation chain transfer process (RAFT)[1−7] and macromolecular architecture design by interchange of xanthates (MADIX)[8−10] based radical polymerizations. After polymerization these moieties are preserved at the chain end of the product,[11,12] as indicated by nuclear magnetic resonance spectroscopy (NMR)[13−15] and matrix-assisted laser desorption ionization (MALDI) or electrospray ionization (ESI) mass spectroscopy (MS) results,[16−25] providing further possibility of functionalization and coupling. One of the most important functionalization is the conversion of thiocarbonylthio moiety into thiol group by aminolysis,[26−35] hydrolysis,[36,37] and reduction.[38−40] Direct coupling of electron-deficient dithioester moieties and appropriate dienes through hetero-Diels−Alder reaction has been developed to synthesize block and star (co)polymers.[41−43] The oxidation of dithioester termini into thioesters, either by peroxides[16] or by air in the presence of radical,[44] has also been observed. The oxidation has been used to convert RAFT polymerization products into polymers with hydroxyl termini.[45] The end functionalization of RAFT polymerization products has been highlighted in comprehensive reviews very recently.[46−48]

Thermal decomposition of RAFT agent has been observed some years ago and has caused attention with the aim of end group removal to stabilize the RAFT polymerization products.[34,49−55] The decomposition also closely relates to the fidelity of the thiocarbonythio chain ends and therefore to the efficiencies of end functionlization and block copolymerization. If decomposition occurs during the polymerization, it will cause retardation to polymerization rate[56,57] through the loss of the living chain end and subsequent radical quenching by the resulting dithiocarboxylic acid, in resemblance to the retardation caused by the hydrolysis of,[58] or impurities in,[59,60] the RAFT/MADIX agents. The primary pathway of thermal decomposition is through Chugaev-like elimination,[61−65] in which thiocarbonylthio moiety and a

Received: July 10, 2011
Revised: September 14, 2011
Published: October 04, 2011

β-hydrogen are expelled, resulting in unsaturated species[34,52−57,66] and the corresponding acids.[52−54,56,66]

Homolytic decomposition generating a thiocarbonylthio radical and a leaving group-derived radical has also been proposed for polystyrene,[55] poly(methyl methacrylate) (PMMA), and poly(butyl acrylate) (PBA)[52,54] prepared by trithiocarbonate-mediated polymerization. In that case, the leaving propagating radical may undergo chain end backbiting followed by β-scission, resulting in short chain species. In the case of PMMA, depolymerization from the leaving radical, releasing MMA monomer, has been observed. In another study of thermolysis by GC-MS and TGA,[67] it has been found that the carbon−sulfur single bond is the most labile and is affected by the structure of Z- and R-substituents of the agents.

In the present work, a series of RAFT/MADIX agents are subject to thermal decomposition in solution. The experimental conditions are more close to large-scale post-treatment than thermolysis in TGA instrument to remove the sulfur-containing chain end. Where necessary, the decomposition products are isolated and characterized. Therefore, it is possible to discuss the reaction mechanism in the light of final products instead of transient species as those in thermolysis. The relationship between the thermal stabilities and molecular structures of thiocarbonythio compounds are investigated with respect to the reaction mechanism and discussed in correlation with the chain transfer activity measured by the CSIRO group[68,69] and with the stability of RAFT agents calculated by Coote using *ab initio* calculation.[70−74] In addition, the thermal stability of a universal RAFT agent[75] at the neutral and protonated states is also investigated.

EXPERIMENTAL SECTION

Materials. α,α'-Azobis(isobutyronitrile) (AIBN, Shanghai 4th Factory of Chemicals, 99%) was recrystallized from methanol. Methanol (Lingfeng Chemicals, 99.5%), petroleum ether (60−90 °C range, Shenxiang Chemicals, 99%), and dichloromethane (Lingfeng Chemicals, 99%) were dried over $CaCl_2$ and distilled before use. Carbon disulfide (CS_2, Shanghai 4th Factory of Chemicals, 99%) was purified by vigorously shaking with $KMnO_4$ (0.4 wt % based on CS_2) followed by filtration and distillation to collect a colorless fraction. Cyclohexane (Feida, 99.5%), benzene (Shenxiang Chemicals, 99%), tetrahydrofuran (Shanghai Qiangsheng Chemicals, 99%), and toluene (Lingfeng Chemicals, 99%) were dried over sodium and distilled before use. *tert*-Butylbenzene (Aldrich, 99%), diphenyl ether (Acros, 99%), ethyl α-bromoisobutyrate (Aldrich, 98%), DMSO (Aladdin, HPLC grade), and *p*-toluenesulfonic acid monohydrate (Aldrich, 98.5%) were used as received. Methyl methacrylate (MMA, Shanghai 4th Factory of Chemicals, 98%) and styrene (Yonghua Special Chemicals, 99%) were distilled after being stirred over CaH_2 for 24 h.

Measurements. High-pressure liquid chromatography (HPLC) was performed on an instrument composed of a Waters 515 pump, a C-18 column, and a UV detector with the wavelength set at 254 and 300 nm. Acetonitrile/water (v/v = 83/17) mixture was used as eluent (1.0 mL/min) at 40 °C. ^{1}H and ^{13}C NMR and HSQC measurements were carried out on a Bruker (500 MHz) NMR instrument, using tetramethylsilane (TMS) as the interior reference. Gel permeation chromatography (GPC) was performed on a Waters 410 system equipped with a guard column and three TSK columns (TSK Gel H-type, pore size 15, 30, and 200 Å) in series, a Waters 410 RI, and a Waters 486 UV detector, using THF as the eluent at a flow rate of 1 mL/min at 40 °C. The columns were calibrated by narrow polystyrene standard with molecular weight ranging from 2.2×10^3 to 5.2×10^5 g/mol. Gas chromatography−mass spectrometry (GC-MS) was performed on an Agilent Technologies 6890N system, equipped with a mass-selective detector using electron impact ionization. Analytes were separated by a HP-5MS capillary column of 30 m (0.25 i.d. and 0.25 μm film thickness), which was inserted directly into the ion source of the MS system. Helium (99.999%) was the carrier gas maintained at a flow rate of 1.0 mL/min. The injector was kept at 280 °C, and samples were split injected (1 μL, split ratio 100:1). The column oven temperature was programmed to start at 80 °C for 2 min, ramp at 10 °C/min to 280 °C, and held at 280 °C for 5 min. EI spectra were scanned between 50 and 550 Da in the full-scan acquisition mode. The transfer line and EI source temperature were both 230 °C. The electron multiplier voltage was set on 70 eV. Matrix-assisted laser desorption ionization time-of-flight mass spectroscopy (MALDI-TOF MS) measurements were performed on a Voyager-DE STR (Applied Biosystems, Framingham, MA) equipped with a nitrogen laser emitting at 337 nm with a 3 ns pulse duration. The instrument was calibrated with angiotensin and insulin and operated in the reflector mode. The accelerating potential is 20 kV. For each spectrum, 1000 laser shots were accumulated. The matrix used was (*R*)-cyano-4-hydroxycinnamic acid (CHCA). Samples were prepared by mixing the solution of polymer (2 μL, 10 mg/mL in THF), the matrix (10 μL, 20 mg/mL in THF), and silver trifluoroacetate (TFA, cationizing agent, 1 μL, 10 mg/mL in THF). An aliquot of 1 μL of the resulting mixture was spotted on the target plate and air-dried. Element analysis was carried on a Heraeus 1106 instrument.

Synthesis of the RAFT/MADIX Agents. For the synthetic procedures of agents which have been reported, the readers refer to the corresponding literature indicated in the following. The characterization results of all agents are presented.

*Cumyl Dithiobenzoate (**1**).* The synthesis follows that in ref 76. The product is purple crystals. ^{1}H NMR ($CDCl_3$): δ (ppm) = 2.00 (s, 6H, CH_3−C−CH_3), 7.85 (d, 2H, *o*-Ar*H* of dithiobenzoate), 7.46 (dd, 1H, *p*-Ar*H* of dithiobenzoate), 7.55 (d, 2H, *o*-Ar*H*), 7.22(dd, 1H, *p*-Ar*H*), 7.31−7.39 (m, 4H, Ar*H*). FT-IR: ν (cm^{-1}) = 1218 and 1042 (C═S). UV−vis max (cyclohexane): 299 and 444 nm. GC-MS (EI): *m*/*e* = 272. Purity by HPLC = 99.0%.

*1-Phenylethyl Dithiobenzoate (**2**).* The synthesis follows that in ref 76. The product is red crystals. ^{1}H NMR ($CDCl_3$): δ (ppm) = 1.81 (d, 3H, CH−CH_3), 5.26 (q, 1H, C*H*−CH_3), 7.95 (d, 2H, *o*-Ar*H* of dithiobenzoate), 7.50 (dd, 1H, *p*-Ar*H* of dithiobenzoate), 7.25−7.45 (m, 7H, Ar*H*), FT-IR: ν (cm^{-1}) = 1225 and 1042 (C═S). UV−vis max (cyclohexane): 298 and 500 nm. GC-MS (EI): *m*/*e* = 258. Purity by HPLC = 99.2%.

*1-Phenylethyl 4-Nitrobenzodithioate (**3**).* 1-(Bromomethyl)-4-nitrobenzene (21.60 g, 0.10 mol), sulfur (7.05 g, 0.22 mol) and triethylamine (40 mL) were added to a round bottom flask. Then, 1-bromoethylbenzene (20.36 g, 0.11 mol) and DMF (130 mL) were added dropwise over one hour to the flask. The mixture was then warmed at 60 C for 12 h with magnetic stirring. The mixture was filtered. The obtained solution was condensed by evaporation of DMF. The crude product was purified by column chromatography on silica using petroleum ether as eluent to obtain a purple oil. ^{1}H NMR ($CDCl_3$): δ (ppm) = 1.83 (d, 3H, CH−CH_3), 5.21 (q, 1H, C*H*−CH_3), 7.31 (t, 1H, *p*-Ar*H*), 7.36 (t, 2H, *m*-Ar*H*), 7.43 (d, 2H, *o*-Ar*H*), 8.02 (d, 2H, *o*-Ar*H* of dithiobenzoate), 8.20 (d, 2H, *m*-Ar*H* of dithiobenzoate). FT-IR: ν (cm^{-1}) = 1062 and 1220 cm^{-1} (C═S). UV−vis max (cyclohexane): 297 and 519 nm. Purity by HPLC = 99.0%.

*1-Phenylethyl Phenyldithioacetate (**4**).* The synthesis follows that in ref 77. The product is fine yellow crystals. ^{1}H NMR ($CDCl_3$): δ (ppm) = 1.68 (d, 3H, CH−CH_3), 5.05 (q, 1H, C*H*−CH_3), 4.26 (s, 2H, CH_2−Ph), 7.17−7.35 (m, 10H, Ar*H*). FT-IR: ν (cm^{-1}) = 1219 and 1037 (C═S). UV−vis max (cyclohexane): 308 nm. GC-MS (EI): *m*/*e* = 272. Purity by HPLC = 99.0%.

*Benzyl Dithiobenzoate (**5**).* The synthesis follows that in ref 76. The product is red oil. ^{1}H NMR ($CDCl_3$): δ (ppm) = 4.6 (s, 2H, CH_2−Ph), 8.00 (d, 2H, *o*-Ar*H* of dithiobenzoate), 7.53 (dd, 1H, *p*-Ar*H* of dithiobenzoate), 7.25−7.45 (m, 7H, Ar*H*). FT-IR: ν (cm^{-1}) = 1226 and 1044 (C═S). UV−vis max (cyclohexane): 302 and 504 nm. GC-MS (EI): *m*/*e* = 244. Purity by HPLC = 99.4%.

Table 1. Results of Thermal Decomposition Reaction of RAFT/MADIX Agents

No.	RAFT/MADIX agents	Decomposition Product	Solvent	E_{act} (KJ/mol)	$\ln A_d$ ($L\ mol^{-1}s^{-1}$)	$k_{dec,333}$[a] /s^{-1}
1[b]	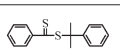		*t*-butylbenzene	107.0 (103.2)	22.8 (21.6)	1.27×10^{-7} (1.67×10^{-7})
2	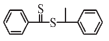		*t*-butylbenzene	77.6	10.2	1.84×10^{-8}
3	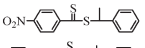		diphenyl ether	58.6	5.72	1.93×10^{-7}
4	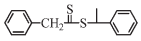		*t*-butylbenzene	61.8	5.94	7.66×10^{-8}
5	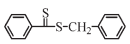		diphenyl ether	181.5	33.9	1.69×10^{-14}
6	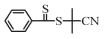		*t*-butylbenzene	45.8	3.67	2.57×10^{-6}
7	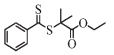		*t*-butylbenzene	65.2	7.37	9.41×10^{-8}
8	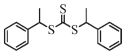		diphenyl ether	113.9	21.0	1.78×10^{-9}
9	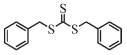		diphenyl ether	137.6	22.4	1.45×10^{-12}
10	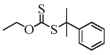		*t*-butylbenzene	94.7	17.5	5.93×10^{-8}
11	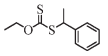		diphenyl ether	148.5	28.1	8.22×10^{-12}
12	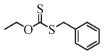	$H_2C{=}CH_2$[c]	diphenyl ether	149.5	26.9	1.60×10^{-12}
13			diphenyl ether	132.2	25.2	1.63×10^{-10}
14	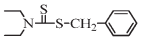	no reaction	diphenyl ether	—	—	—
15	PS-RAFT	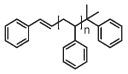	*t*-butylbenzene	90.3	13.9	7.35×10^{-9}
16	PMMA-RAFT	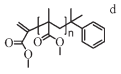 [d]	*t*-butylbenzene	77.6	13.8	7.10×10^{-7}
17			diphenyl ether	154.7	27.4	4.36×10^{-13}
18		—[e]	DMSO	116.1	22.7	4.43×10^{-9}

[a] $k_{dec,333}$ is the calculated apparent rate coefficient of thermal decomposition at 333 K. [b] The results are from ref 66, in which k_{dec} at 333 K was erroneously calculated as $4.64\times10^{-5}\ s^{-1}$. The numbers in parentheses are average values from three parallel experiments. [c] Expected product according to ref 61. [d] Expected product according to refs 53 and 56. [e] ^{1}H NMR spectrum of the reaction mixture is given in the next section.

*2-Cyanoprop-2-yl Dithiobenzoate (**6**).* The synthesis follows that in ref 78. The product is pink oil. ^{1}H NMR ($CDCl_3$): δ (ppm) = 1.95 (s, 6H, CH_3−C−CH_3), 7.92 (d, 2H, *o*-Ar*H* of dithiobenzoate), 7.56(dd, 1H, *p*-Ar*H* of dithiobenzoate), 7.40 (dd, 2H, *m*-Ar*H* of dithiobenzoate). FT-IR: ν (cm^{-1}) = 1229 and 1047 (C═S); ν (cm^{-1}) = 2231(CN). UV−vis max (cyclohexane): 296 and 529 nm. GC-MS (EI): m/e = 221. Purity by HPLC = 99.0%.

*2-(Ethoxycarbonyl)prop-2-yl Dithiobenzoate (**7**).* The synthesis follows that in ref 31. The product is red oil. ^{1}H NMR ($CDCl_3$): δ (ppm) = 1.24 (t, 3H, CH_2−CH_3), 1.76 (s, 6H, CH_3−C−CH_3), 4.16 (q, 2H, O−$CH_2$$CH_3$), 7.35 (dd, 2H, *m*-Ar*H* of dithiobenzoate), 7.52 (dd, 1H, *p*-Ar*H* of dithiobenzoate), 7.95 (d, 2H, *o*-Ar*H* of dithiobenzoate). FT-IR: ν (cm^{-1}) = 1260 and 1042 (C═S); ν (cm^{-1}) = 1732 (C═O). UV−vis max (cyclohexane): 296 and 513 nm. GC-MS (EI): m/e = 268. Purity by HPLC = 99.8%.

*Bis(1-phenylethyl) Trithiocarbonate (**8**).* The synthesis follows that in ref 79. The product is yellow oil. ^{1}H NMR ($CDCl_3$): δ (ppm) = 1.72−1.75 (dd, 6H, CH_3−CH), 5.31 (q, 4H, CH_2−Ph), 7.26−7.36 (m, 20H, Ar*H*). FT-IR: ν (cm^{-1}) 1208 and 1069 (C═S). UV−vis max (cyclohexane): 313 nm. Purity by HPLC = 99.0%.

*Dibenzyl Trithiocarbonate (**9**).* The synthesis follows that in ref 80. The product is yellow oil. ^{1}H NMR: δ (ppm) = 4.62 (s, 4H, CH_2−Ph), 7.26−7.36 (m, 20H, Ar*H*). FT-IR: ν (cm^{-1}) = 1223 and 1063 (C═S). UV−vis max (cyclohexane): 307 nm. GC-MS (EI): m/e = 290. Purity by HPLC = 99.5%.

*O-Ethyl S-(2-Phenylpropan-2-yl)xanthate (**10**).* The synthesis follows that in ref 81. The product is white crystals. ^{1}H NMR ($CDCl_3$): δ (ppm) = 1.82 (s, 6H, CH_3-C-CH_3), 4.38 (q, 2H, CH_3−CH_2), 1.06 (t, 3H, CH_3−CH_2), 7.52 (d, 1H, *o*-Ar*H*), 7.31 (dd, 2H, *m*-Ar*H*), 7.22 (dd, 2H, *p*-Ar*H*). FT-IR: ν (cm^{-1}) = 1238 and 1042 (C═S). UV−vis max (cyclohexane): 286 nm. Purity by HPLC = 98.6%.

*O-Ethyl S-(1-phenylethyl)xanthate (**11**).* The synthesis follows that in ref 81. The product is pale yellow oil. ^{1}H NMR ($CDCl_3$): δ (ppm) = 1.71 (d, 3H, CH−CH_3), 4.89 (q, H, C*H*−CH_3), 4.61 (q, 2H, CH_3−CH_2), 1.38 (t, 3H, CH_3−CH_2), 7.37 (d, 2H, *o*-Ar*H*), 7.31 (dd, 2H, *m*-Ar*H*), 7.25 (dd, H, *p*-Ar*H*). FT-IR: ν (cm^{-1}) = 1213 and 1041 (C═S).

dx.doi.org/10.1021/ma201570f |*Macromolecules* 2011, 44, 8446–8457

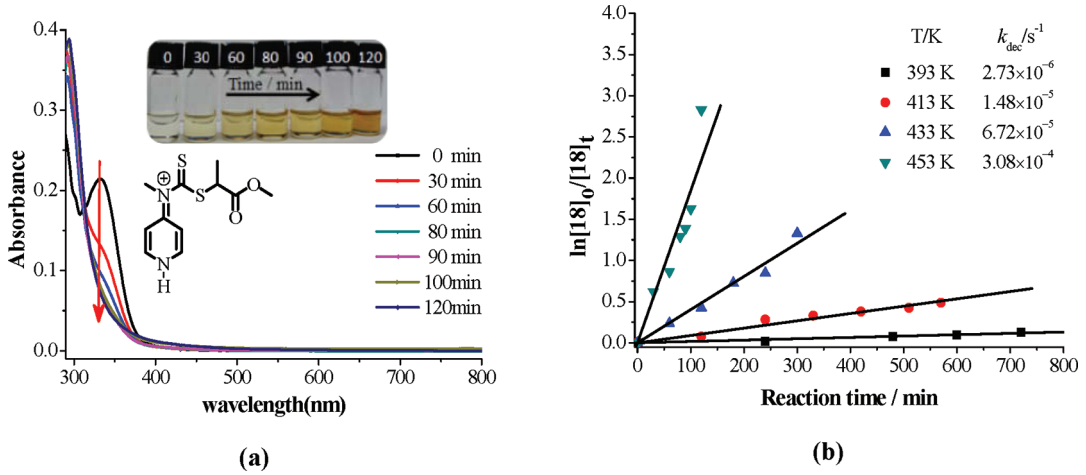

Figure 1. (a) UV−vis spectra following the thermal decomposition reaction of protonated 1-methoxycarbonylethyl *N*-methyl-*N*-pyridin-4-yldithiocarbamate (**18**), (0.0135 g, 5.00 × 10^{-2} mmol) in DMSO (5 mL) at 180 °C (inset: photographs showing the color change during heating) and (b) kinetic plots of heating **18** at different temperatures: ■, 393 K; ●, 413 K; ▲, 433 K; ▼, 453 K.

GC-MS (EI): m/e = 226. UV−vis max (cyclohexane): 283 nm. Purity by HPLC = 99.0%.

O-Ethyl S-Benzylxanthate (**12**). The synthesis follows that in ref 79. The product is pale yellow oil. ^{1}H NMR ($CDCl_3$): δ (ppm) = 4.37 (s, 2H, CH_2−Ar), 4.65 (q, 2H, CH_3−CH_2), 1.42 (t, 3H, CH_3−CH_2), 7.25−7.35 (m, 5H, Ar*H*). FT-IR: ν (cm^{-1}) = 1216 and 1047 (C═S). GC-MS (EI): m/e = 212. UV−vis max (cyclohexane): 279 nm. Purity by HPLC = 99.8%.

1-Phenylethyl-N,N′-diethyldithiocarbamate (**13**). The synthesis follows that in ref 82. The product is pale yellow oil. ^{1}H NMR ($CDCl_3$): δ (ppm) = 1.24 and 1.27 (t, 6H, CH_2−CH_3), 1.78 (d, 3H, CH−CH_3), 3.70 and 4.02 (q, 4H, CH_2−CH_3), 5.27 (q, H, C*H*−CH_3), 7.25−7.43 (m, 5H, Ar*H*). FT-IR: ν (cm^{-1}) = 1208 and 1069 (C═S). GC-MS (EI): m/e = 253. UV−vis max (cyclohexane): 283 nm. Purity by HPLC = 99.5%.

Benzyl-N,N′-diethyldithicarbamate (**14**). The synthesis follows that in ref 82. The product is pale yellow oil. ^{1}H NMR ($CDCl_3$): δ (ppm) = 1.26 and 1.29 (t, 6H, CH_2−CH_3), 3.72 and 4.04 (q, 4H, CH_2−CH_3), 4.54 (s, 2H, CH_2−Ar), 7.25−7.38 (m, 5H, Ar*H*). FT-IR: ν (cm^{-1}) = 1208 and 1069 (C═S). GC-MS (EI): m/e = 239. UV−vis max (cyclohexane): 280 nm. Purity by HPLC = 99.9%.

PS with Dithiobenzoate Terminus (**15**). Styrene (8.87 g, 0.09 mol) bulk polymerization, initiated by AIBN (0.03 g, 0.20 mmol), was carried out in the presence of CDB (0.11 g, 6.41 mmol) in a 50 mL flask under argon at 60 °C for 10 h. The resulting PS-RAFT was obtained as a pink powder after three times of dissolving in THF and precipitating from methanol. The product was analyzed by GPC. Number-average molecular weight: $M_{n,GPC}$ = 2600 g/mol, PDI = 1.10.

PMMA with Dithiobenzoate Terminus (**16**). Methyl methacrylate (MMA) (6.20 g, 0.06 mol) polymerization, initiated by AIBN (0.16 g, 0.97 mmol), was carried out in the presence of CDB (0.57 g, 2.10 mmol) in benzene (16 mL) under argon at 60 °C for 8 h. PMMA-RAFT was obtained as a pink powder after three times of dissolving in THF and precipitating from petroleum ether. The product was analyzed by GPC. Number-average molecular weight: $M_{n,GPC}$ = 2800 g/mol, PDI = 1.14.

1-Methoxycarbonylethyl-N-methyl-N-pyridin-4-yldithiocarbamate (**17**). The synthesis follows that in ref 75. The product is off-white solid. ^{1}H NMR ($CDCl_3$): δ (ppm) = 1.53 (d, 3H, CHCH_3); 3.73 (s, 6H, COOCH_3 and N−CH_3); 4.65 (q, 1H, C*H*CH$_3$); 7.30 (d, 2H, *m*-Ar*H*); 8.75 (br s, 2H, *o*-Ar*H*). FT-IR: ν (cm^{-1}) = 1226 and 1094 (C═S). GC-MS (EI): m/e = 270. UV−vis max (cyclohexane): 296 nm. Purity by HPLC = 99.0%.

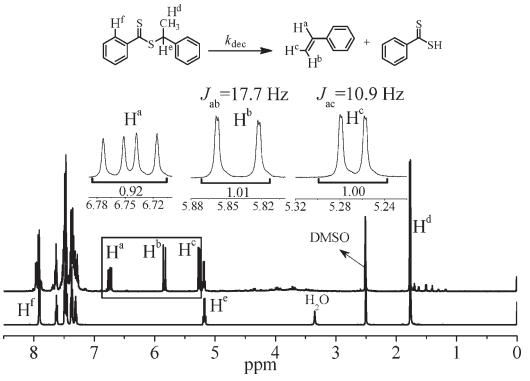

Figure 2. ^{1}H NMR spectra of the reaction mixture of heating 1-phenylethyl dithiobenzoate (**2**) at 160 °C in DMSO-d_6 (upper, 18 h; lower, 0 h).

Protonation of 17 with TsOH (**18**). The synthesis follows that in ref 75. The product is yellow solid. ^{1}H NMR (DMSO-d_6): δ (ppm) = 1.53 (d, 3H, CHCH_3); 2.33 (s, 3H, *p*-toluenesulfonate, CH_3); 3.70, 3.75 (s, 6H,COOCH_3 and N−CH_3); 4.57 (q, 1H, C*H*CH$_3$); 7.14 (d, 2H, *p*-toluenesulfonate *m*-Ar*H*); 7.73 (d, 2H, *p*-toluenesulfonate *o*-Ar*H*); 7.90 (d, 2H, *m*-Ar*H*); 8.94 (d, 2H, *o*-Ar*H*).

Thermal Decomposition of RAFT/MADIX Agents. RAFT/MADIX agent (listed in Table 1) was dissolved in *tert*-butylbenzene, diphenyl ether, or DMSO in a 5 mL flask, keeping the initial concentration ca. 0.01 mol L^{-1}. Then the reaction mixture was transferred to individual ampules (∼1 mL) and deaerated through three cycles of freezing−pumping−thawing. The sealed ampules were then placed in an oil bath. Each ampule was removed after a predetermined time interval. The reactions were stopped by quenching into liquid nitrogen. The concentration of the starting material was measured by HPLC detected at 254 or 300 nm.

RESULTS AND DISCUSSION

Mechanism of Thermal Decomposition. Thermal decomposition reactions are performed by heating the RAFT/MADIX agents in well-deaerated solution of *tert*-butylbenzene, diphenyl ether, or DMSO-d_6. The products are characterized by at least one method of HPLC, NMR, or MALDI-TOF MS. Appropriate temperatures are applied for each compound due to different

dx.doi.org/10.1021/ma201570f |*Macromolecules* 2011, 44, 8446–8457

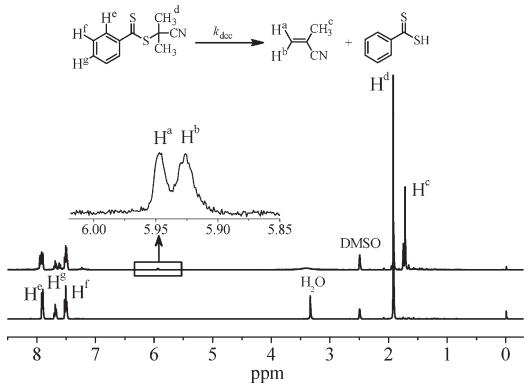

Figure 3. ^{1}H NMR spectra of the reaction mixture of heating 2-cyanoisopropyl dithiobenzoate (**6**) at 160 °C in DMSO-d_6 (upper, 3 h; lower, 0 h).

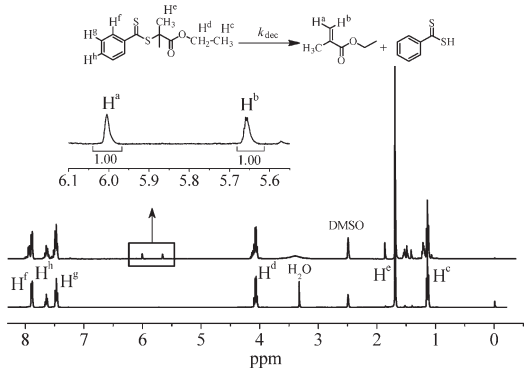

Figure 4. ^{1}H NMR spectra of the reaction mixture of heating 2--(ethoxycarbonyl)prop-2-yl dithiobenzoate (**7**) at 160 °C in DMSO-d_6 (upper, 1.5 h; lower, 0 h).

stabilities. The kinetic results are measured by HPLC, meanwhile all reactions are also followed by UV−vis. An example of heating protonated 1-methoxycarbonylethyl *N*-methyl-*N*-pyridin-4-yl-dithiocarbamate, **18** (the universal RAFT agents in the protonated form in Table 1), is shown in Figure 1, in which the intensity of the absorption band of thiocarbonylthio moiety at 330 nm of **18** decreases along with reaction time.

Four classes of RAFT/MADIX agents, e.g., dithioesters, trithiocarbonates, xanthates, and dithiocarbamates, are investigated. The results are listed in Table 1. In most cases the main products are olefins formed from Chugaev-like elimination, provided that there is β-hydrogen in the molecule. For example, dithioester **1**[66] and xanthate **10** release α-methylstyrene upon heating (HPLC in Supporting Information) because they both possess cumyl substituent as the leaving group. Similarly, those possessing 1-phenylethyl leaving group, such as dithioester **2**, **3**, **4**, trithiocarbonate **8**, xanthate **11**, and dithiocarbamate **13**, yields styrene which is observed by HPLC (RT = 4.40 min, Supporting Information). NMR spectra of the reaction mixture of **2** during heating are shown in Figure 2, in which signals of vinylic protons in the product, styrene, are observed at chemical shifts δ = 5.27, 5.84, and 6.75 ppm. The ratio of integrations (data underneath the peaks in the inset) and the splitting constant agree well with the structure of styrene.

Compound **6**, with the leaving group derived from AIBN, releases α-methylacrylonitrile, of which the vinylic and α-methyl protons appear at δ = 5.94 ppm (doublet) and 1.73 ppm (Figure 3). Compound **7**, resembling the living chain in methacrylate RAFT polymerization, decomposes into ethyl methacrylate. The vinylic protons give signals at δ = 5.65 and 6.00 ppm as shown in Figure 4.

On the other hand, dithioester **5** and trithiocarbonate **9** possessing benzyl as the leaving group (no β-hydrogen) are not able to decompose through Chugaev process. Both **5** and **9** yield stilbene in pure (*E*)-isomer as the main product. The characterizations of the isolated product using ^{1}H and ^{13}C NMR are shown in Figure 5. The vinylic protons give signal at δ = 7.10 ppm, while aromatic protons give signals at δ = 7.24, 7.38, and 7.50 ppm, which are typical for (*E*)-stilbene.[83] In ^{13}C NMR, the vinylic carbon is observed at δ = 126 ppm. The product is also analyzed by GC-MS (Supporting Information), showing molecular ion at m/z = 180. In addition, both of these reactions release H_2S as detected by $Pb(OAC)_2$.

The elimination of trithiocarbonate or carbonylthiocarbonate to form alkene is well documented.[84−88] Nevertheless, those syntheses usually started from cyclic trithiocarbonate precursors and underwent the 1,2-elimination process. It should be noted that the thermal decomposition of **5** and **9** in the present work forms new C═C bond derived from benzyl groups. The process is more likely to involve a carbene intermediate which is formed by α-elimination on the methylene, as shown in Scheme 1. The first step is the leaving of a proton, possibly aided by the solvent, diphenyl ether, a weak base, and then the leaving of dithiocarboxylic or trithiocarbonic anion to form benzylic carbene, **5-2**. The carbene species is very active and can insert into the C−H bond of the starting material, forming a coupled precursor, **5-3**, which will undergo further β-elimination to form stilbene. The two-step process, e.g., the formation of precursor and subsequent formation of stilbene, resembles the process in the preparation of poly(phenylenevinylene) (PPV) derivatives from xylene-type precursors of xanthate[89,90] and dithiocarbamate.[91−96] However, it is believed that PPV synthesis involves a *p*-quinodimethane intermediate[93] derived by delocalization of carbanion on bifunctionalized aromatic ring. Neither **5** nor **9** in the present work is able to form such an intermediate. The stereoselectivity comes from the second step, in which elimination takes place only between thiocarbonylthio and *cis* β-hydrogen. Thus, for the three conformers of **5-3** (Scheme 1), the most favored is **5-3-a** whereas the energy barrier of **5-3-b** is high and **5-3-c** does not have *cis* β-hydrogen. This leads to the predominant formation of the *E*-isomer of stilbene. The release of H_2S may be a consequence of possible anhydridization between the resulting dithiobenzoic acids.

Trithiocarbonate **9** may undergo not only similar process as in Scheme 1 but also another possible pathway, e.g., the extrusion of CS_2 to form a dibenzyl sulfur ether intermediate, which will further release H_2S to form (*E*)-stilbene (Scheme 2).[97] This is supported by the evidence of sulfur ether species in GC-MS of **9** (Supporting Information).

Xanthate **12** also possesses benzyl as the leaving group but tends to decomposes from the *O*-ethyl side, releasing ethylene and COS according to Chugaev elimination (Scheme 3).[98] This reaction should be in competition with α-elimination on the *S*-benzyl side, which would otherwise result in (*E*)-stilbene. However, no stilbene has been detected by HPLC (Supporting Information). Therefore, Chugaev elimination on *O*-ethyl side

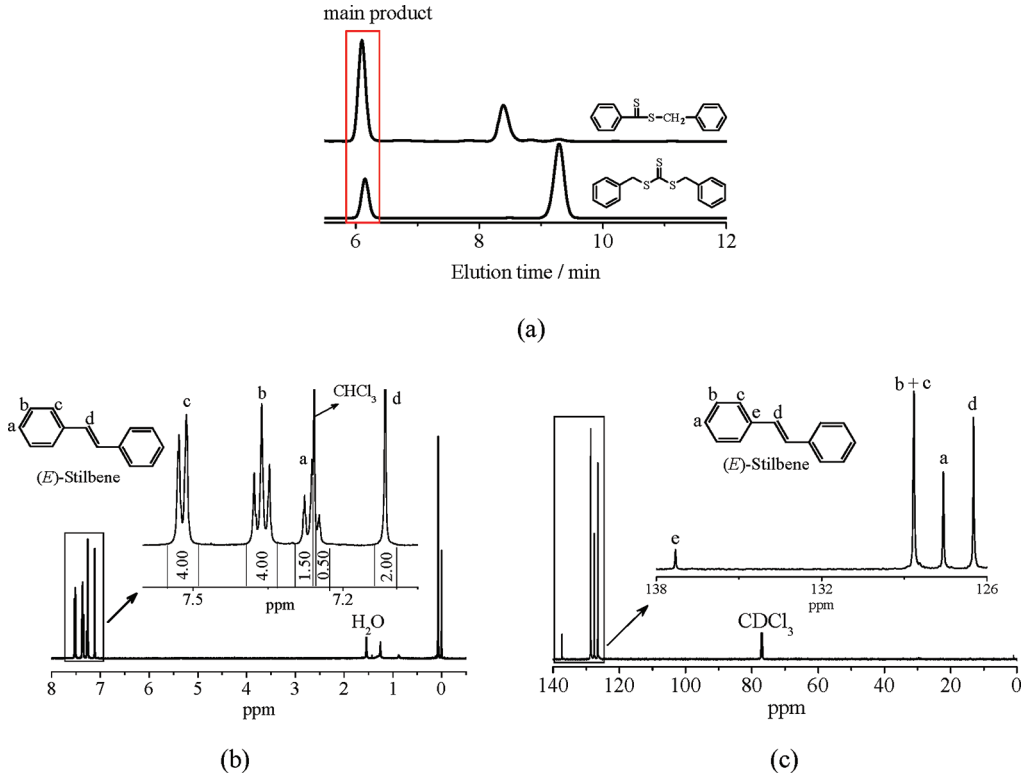

Figure 5. (a) HPLC diagrams of the reaction mixtures of heating dibenzyl trithiocarbonate (**9**) (0.0145 g, 4.99×10^{-2} mmol) and benzyl dithiobenzoate (**5**) (0.0122 g, 4.99×10^{-2} mmol), respectively, in diphenyl ether (5 mL). The main products indicated in the red frame are isolated and characterized using ^{1}H (b) and ^{13}C (c) NMR, which are assignable to (*E*)-stilbene.

Scheme 1. Proposed Mechanism of Decomposition Pathway of Benzyl Dithiobenzoate (5) and the Formation of (*E*)-Stilbene

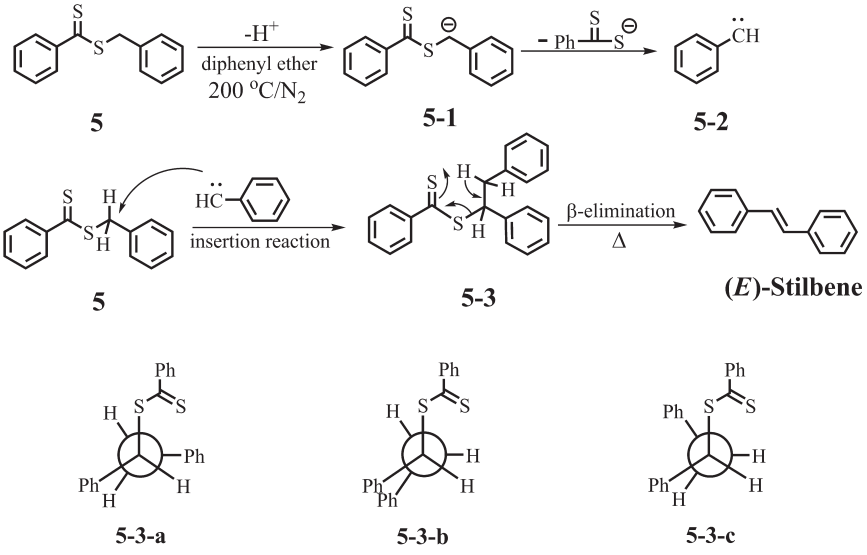

is predominant. Dithiocarbamate **14** is stable up to 240 °C for 30 min without any hint of decomposition, although the leaving group is benzyl as well.

Polystyrenyl dithiobenzoate, **15**, decomposes to give polystyrene with an unsaturated terminus as detected by MALDI-TOF MS of the product precipitated from methanol (Figure 6). The main series of the peaks, P_1 (m/z = 2518.3 in the enlarged spectrum), and a minor series, P_4 (m/z = 2570.3), are assignable to polystyrene chains with ω-unsaturated terminus and two kinds of α-termini, e.g., cumyl derived from the RAFT agents and cyanoisopropyl from AIBN, respectively. Thus, dithioester **15** undergoes the same elimination process as trithiocarbonate

dx.doi.org/10.1021/ma201570f |*Macromolecules* 2011, 44, 8446–8457

from polystyrene chain.[55] The peak at m/z = 2533.3 is assignable to coupling product bearing two cumyl termini, while the origin for m/z = 2546.3 is unclear. It is surprising to find the coupling product since its formation requires homolysis at the S−R single bond, which is not the case in the RAFT polymerization. It seems, however, that homolytic decomposition may take place at elevated temperature (200 °C). Indeed, clear decrease in molecular weight is observed by GPC results for PS-RAFT after heating, which may be ascribed to depolymerization from the resulting propagating radical (Supporting Information). Thermal elimination of PMMA prepared by RAFT polymerization has already been studied in great detail in the literature.[28,29,53,56]

Recently, the CSIRO group reported *N*-(4-pyridinyl)-*N*-methyl dithiocarbamates as a new class of universal RAFT agents to provide excellent control on both active monomer such as styrene and MMA and less active monomer such as vinyl acetate and *N*-vinylpyrolidinone, using protonation−deprotonation switches on pyridinyl ring and the adjacent nitrogen atom.[75] Dithiocarbamate **17**, as well as its protonated form **18**, is one example of the switchable RAFT agents. It is interesting to find from Figure 7 that the main decomposition product from universal RAFT agent is a thiolactone species **19** (RT = 3.27 min, P_1 in HPLC diagram). The ^{1}H NMR spectrum shows two doublets at δ = 7.44 and 8.68 ppm, which are assignable to protons on pyridine ring, while singlets at δ = 3.46 and 2.12 ppm are for methyl groups, respectively. These signals show the expected ratio of integration, 2:2:3:3. In the ^{13}C NMR spectrum, the signals for thiocarbonyl and carbonyl are observed at δ = 198 and 177 ppm, respectively. The connections between carbons and protons are confirmed by HSQC measurement. The MS spectrum shows a molecular ion at m/z = 238. In addition, IR spectrum shows strong bands for thiocarbonyl and carbonyl at 1124 and 1728 cm^{-1}, respectively (Supporting Information). Results of element analysis shows the content of C: 49.14%, H: 4.35%, N: 10.71%, and S: 24.48%, which agree well with the expected thiolactone structure **19** (calculated: C: 50.35%, H: 4.24%, N: 11.75%, S: 26.90%).

The formation of **19** may involve a radical process. As shown in Scheme 4, homolysis of **17** generates a thiocarbamoyl radical **17-1** and an alkylthio radical **17-2**. The latter may undergo hydride migration and then cyclization to form radical **17-3**, which will recombine with **17-1** to form thiolactone substituted thiocarbonyl amide **19**. Since there is no vinylic protons observable in ^{1}H NMR (Supporting Information), the decomposition of **17** is not through Chugaev elimination, although it possess β-hydrogen. This unusual property clearly indicates the high stability of the S−R single bond caused by the lone pair donating ability of the nitrogen. Marginal stabilization of **17** may also be imparted by the canonical structure between nitrogen and the pyridinyl ring.

It is therefore summarized that the decomposition mechanism of the RAFT agents is dominated by the structure of the leaving group. When there is β-hydrogen to the thiocarbonylthio moiety, the decomposition proceeds according to Chugaev elimination mechanism. Molecules without β-hydrogen may involve carbene intermediate, which is formed through α-elimination, followed by β-elimination in the second step, although the two steps may occur simultaneously in the whole system. Nevertheless, it should be pointed out that the decomposition may be more complicated, keeping in mind that only main products are analyzed in the present work. Sulfur-containing byproduct, possibly dithiocarboxylic acid and its derivatives, have not been precisely characterized due to the difficulty in obtaining pure substances.

Kinetics of the Thermal Decomposition. Despite the different reaction pathways, the kinetics of the decomposition is investigated by isothermal reaction in solution at different temperatures. For simplification, all the thermal decomposition reactions are regarded as unimolecular process with the ignorance

Scheme 2. An Additional Pathway for the Thermal Decomposition of Dibenzyl Trithiocarbonate (9)

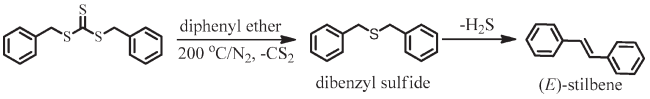

Scheme 3. Chugaev Elimination on *O*-Side of *O*-Ethyl *S*-Benzylxanthate (12)[98]

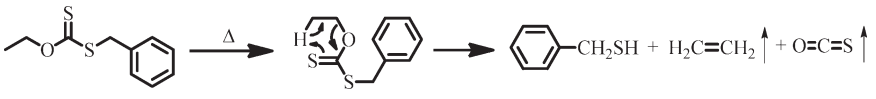

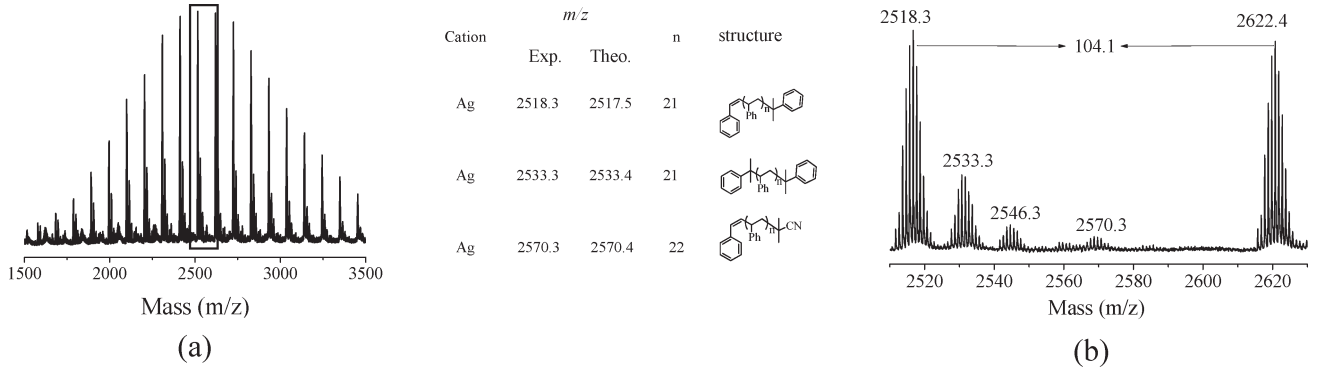

Figure 6. Matrix-assisted laser desorption ionization time-of-flight mass spectrum (MALDI-TOF MS) of thermal decomposition product of PS-RAFT (M_n = 2600 g/mol, M_w/M_n = 1.10) in diphenyl ether at 473 K for 70 h (a: full view; b: partial enlargement).

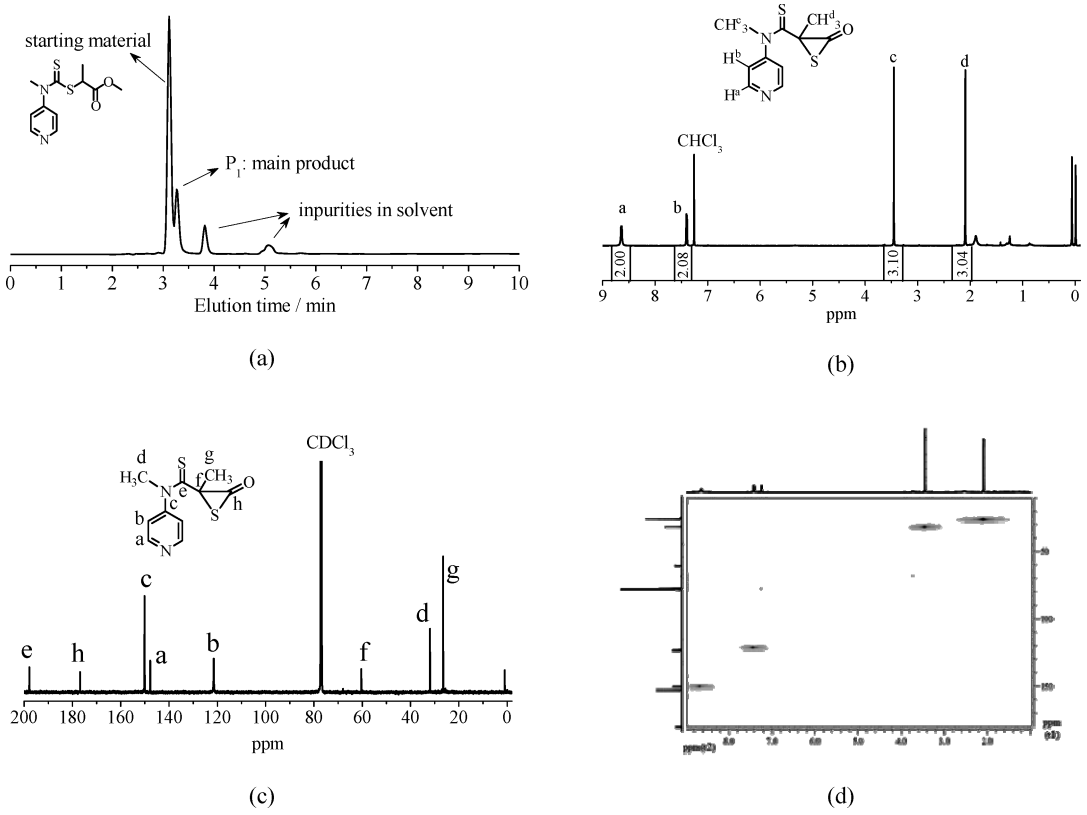

Figure 7. (a) HPLC of the reaction mixture heating 1-methoxycarbonylethyl-*N*-methyl-*N*-pyridin-4-yl dithiocarbamate (universal RAFT agent: **17**) (0.0135 g, 4.99×10^{-2} mmol) in diphenyl ether at 240 °C for 70 min. The main product, P_1, is isolated and characterized by ^{1}H (b) and ^{13}C (c) NMR and HSQC (d).

Scheme 4. Proposed Mechanism of Thermal Decomposition of 1-Methoxycarbonylethyl-*N*-methyl-*N*-pyridin-4-yl Dithiocarbamate (Universal RAFT Agent: 17)

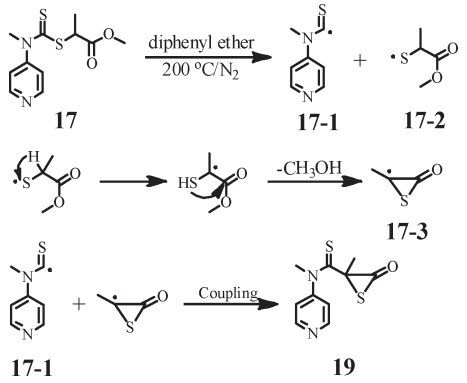

of any reverse reaction. Therefore, the kinetic equation is expressed by eq 1 in which $[ZSSR]_0$ and $[ZSSR]_t$ represent HPLC measured initial and instantaneous concentrations of the RAFT agents and k_{dec} is the apparent decomposition rate coefficient.

$$\ln\left(\frac{[ZSSR]_0}{[ZSSR]_t}\right) = k_{dec}t \qquad (1)$$

The concentrations are plotted against reaction time at different temperatures. One example of heating **18** is shown in Figure 1b. Different values of k_ds are obtained as the slopes of the fitted lines. The activation energy, E_{act}, is obtained from Arrhenius plots, by which the rate coefficient at 333 K, $k_{dec,333}$, can be calculated (Table 1). Standard errors in E_{act} are estimated to be ±2.9 and ±5.9 kJ/mol for **1** and **16**, respectively.

One must be aware, however, that eq 1 expresses only the apparent kinetics. For a number of thiocarbonylthio compounds there could be more decomposition pathways and, therefore, more elementary reactions. The apparent activation energy obtained from the Arrhenius plots is better regarded as the temperature dependence of measured kinetic rate coefficients within the range of performing temperature. The stability of the RAFT agents is discussed in terms of the decomposition rate coefficients at the corresponding temperature, for example, $k_{dec,333}$, at 60 °C.

The Arrhenius plots of various RAFT/MADIX agents are shown in Figure 8, grouped according to the structure of Z- and R-substituents. It appears that the apparent decomposition rate and activation energy depend on both the structures of Z- and R-group. The effect of Z-substituents is inferred by comparison among different classes of thiocarbonylthio compounds, such as **2**, **3**, **4**, **8**, **11**, and **13**, with identical leaving group R = 1-phenylethyl. In the temperature range 100−160 °C, dithioesters **2**, **3**, and **4** readily decompose while the others seems quite stable. The decompositions of **8**, **11**, and **13** are observable only under high temperature, e.g., 200−240 °C, as shown in Figure 8a. In addition, the values of E_{act} of these compounds are larger than those of dithioesters, indicative of larger energy barrier of the reaction intermediate. A subtle effect of the Z-group is also

dx.doi.org/10.1021/ma201570f |*Macromolecules* 2011, 44, 8446–8457

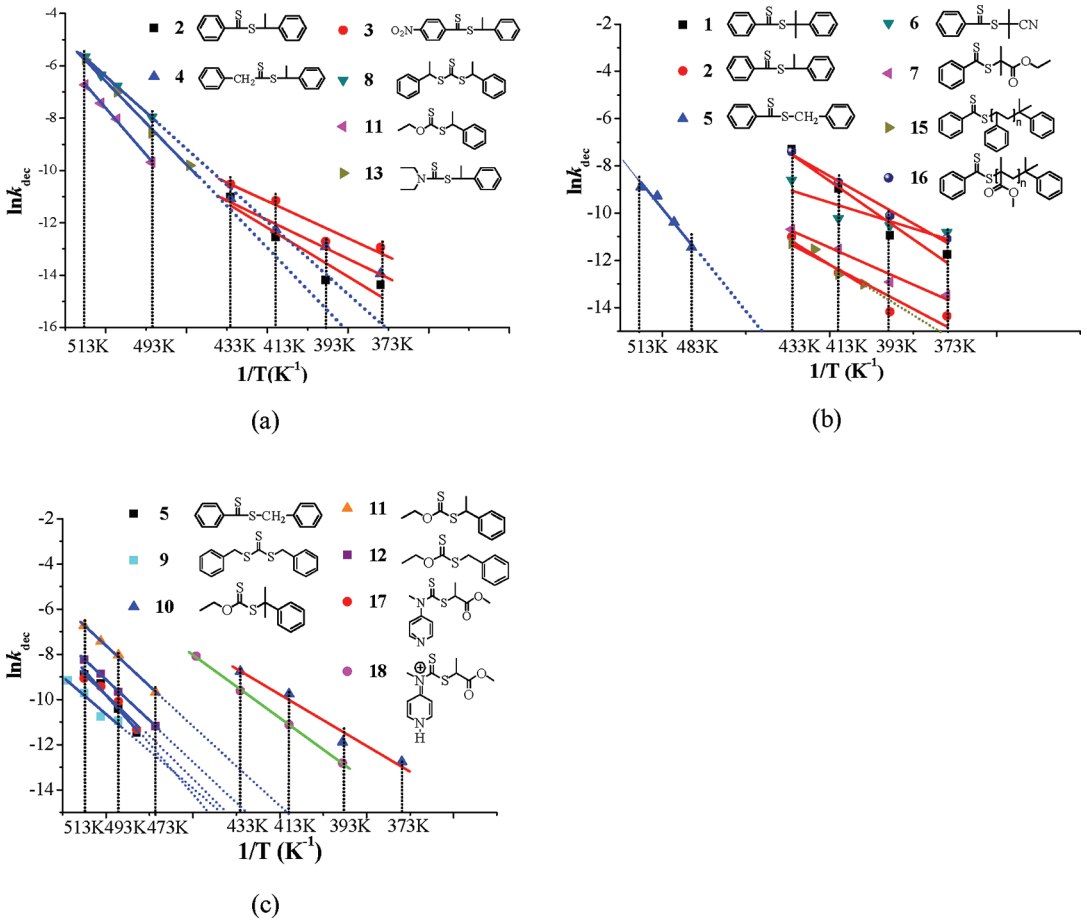

Figure 8. Arrhenius plots of various RAFT/MADIX agents. The dotted extrapolations for systems at higher temperature are drawn only for guiding eyes for comparison. Red lines: heated in *tert*-butylbenzene; blue lines: heated in diphenyl ether; green line: heated in DMSO. The associated values of pre-exponential factor, A_d, and apparent activation energy, E_{act}, are given in Table 1.

Scheme 5. Canonical Structure of the Thiocarbonylthio Compounds

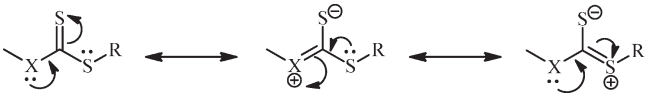

X= O: xanthate;
N: dithiocarbamate;
S: trithiocarbonate.

observed among **2**, **3**, and **4**, in which dithioesters decompose more quickly in the order of Z = −Ph < $-CH_2Ph$ < $-PhNO_2$, although the values of E_{act} are quite close. The overall sequence of stability is as follows: *O*-ethyl (**11**) > $-N(CH_2CH_3)_2$ (**13**) > −SCH (CH_3) Ph (**8**) > −Ph (**2**) > $-CH_2Ph$ (**4**) > $PhNO_2$ (**3**). The sequence correlates well with the order of apparent chain transfer coefficient measured by Rizzardo and co-workers.[68,69] These authors and Coote[70−74] pointed out that lone pair electron donating Z-groups such as alkoxy and dialkylamine stabilize the RAFT agents through resonance between the heteroatom in Z-group and the thiocarbonyl, exerting negative charge on the sulfur atom in the latter. The same effect also exists in estimating the thermal stability of the RAFT/MADIX agents by considering further delocalization of the positive charge between two heteroatoms connected to the thiocarbonyl (Scheme 5). The electron donating nature of the heteroatom favors the resonance isomers by partially canceling the positive charge and thus increases the stability of the compounds. On this basis, electron withdrawing groups tend to destabilize the RAFT/MADIX agents since they cannot lower the energy by conjugation with the partially positive charged atom.

Nevertheless, for those compounds in which the leaving group is benzyl, e.g., **5**, **9**, **12**, and **14**, the decomposition rates increase in the order where Z is $-N(C_2H_5)_2$ (**14**) < −Ph (**5**) < $-SCH_2Ph$ (**9**) < *O*-ethyl (**12**) (vide infra, Figure 8c). This is very different from those with R = 1-phenylethyl. Here, xanthate **12** becomes the most active because it decomposes at *O*-ethyl side. Trithiocarbonate **9** decomposes readily in double pathways as shown in Schemes 1 and 2, thus displaying higher reactivity than dithioester **5** in spite of the presence of electron donating Z-group in **9**. Dithiocarbamate **14** does not show any decomposition under the present conditions.

On the other hand, the effect of R-group is inferred by comparison among various dithioesters with identical Z-group, phenyl (Figure 8b). The thermal stability decreases in the order where R is $-CH_2Ph$ (**5**) > PS− (**15**) > −C(Me)HPh (**2**) > $-C(Me)_2C(=O)OC_2H_5$ (**7**) > $-C(Me)_2Ph$ (**1**) > −PMMA− (**16**) > $-C(Me)_2CN$ (**6**). It is clear that R = benzyl gives the most stable molecule due to specific decomposition mechanism, α-elimination. The stability of those having β-hydrogen is affected

dx.doi.org/10.1021/ma201570f |*Macromolecules* 2011, 44, 8446–8457

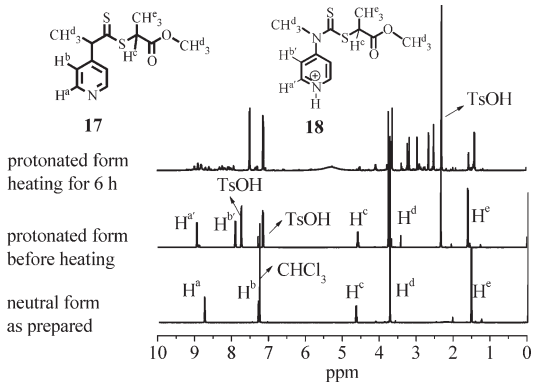

Figure 9. ^{1}H NMR spectra of the reaction mixture of heating protonated form of 1-methoxycarbonylethyl-*N*-methyl-*N*-pyridine-4-yl dithiocarbamate (**18**) at 180 °C in DMSO-d_6 (upper, 6 h; middle, 0 h; lower, as-prepared, 1-methoxycarbonylethyl-*N*-methyl-*N*-pyridine-4-yl dithiocarbamate (universal RAFT agent: **17**).

by statistical, electronic, and steric factors. Statistical factor[98] refers to the probability of conformers that provides *cis* hydrogen to the thiocarbonylthio group, which finally leads to the concerted *cis* elimination. Obviously, more β-hydrogen results in faster elimination reaction. For example, **1** decomposes much faster than **2** because cumyl has three more β-hydrogens than phenylethyl. The same rule seemingly holds for polymeric RAFT agents, PS-RAFT (**15**) and PMMA-RAFT (**16**) with two and five β-hydrogens, respectively. In the latter, there should be two directions for the elimination, e.g., either toward methyl to form 1-olefin or toward methylene to form 2-olefin. The former is predominant. Nonetheless, the ^{1}H NMR spectra in refs 52 and 56 indeed show small peaks both at δ = 5.5 ppm, which are assignable to internal olefinic proton, in addition to those for =CH_2 at δ = 5.5 and 6.2 ppm. The calculated decomposition rate coefficient of **16** at 60 °C is ca. 70 times larger than that of **15** (Table 1). This is the main reason why styrene RAFT polymerization at elevated temperature runs well[99] while MMA may not.

The electronic factor refers to that R-group with electron withdrawing substituent tends to destabilize the RAFT agent because it does not favor the canonical structure in Scheme 5. This has been proved experimentally[68,81] and theoretically[73] by other researchers. Keeping this in mind, it is easy to understand that 2-cyanoisopropyl (**6**) is the most active dithioester. This is because not only the large number of β-hydrogens but also the presence of strong electronic withdrawing cyano group.

Steric factor also contributes to the destabilization effect by weakening the S−R bond through distorted conformation.[73] Nonetheless, it is difficult to distinguish between the steric effect and the statistical factor because more bulky substituents such as cumyl usually has more β-hydrogens. These two factors affect the stability of the thiocarbonylthio compounds in the same direction.

The relationship between R-group and thermal stability is also applicable for xanthates. As shown in Figure 8c, xanthate with R = cumyl (**10**) gives the fastest decomposition rate, followed by those R = 1-phenylethyl (**11**) and benzyl (**12**). The latter decomposes from the *O*-ethyl side due to high stability of the *S*-benzyl single bond.

From Figure 8, it seems that the reaction rate shows stronger temperature dependence in diphenyl ether. The decomposition of **1** is faster in diphenyl ether than in *tert*-butylbenzene within the same temperature range (not shown in the figure), possibly due to the weak basicity of the ether which promotes the elimination of β-hydrogen. However, the apparent activation energy does not show significant difference with each other (102.5 kJ/mol in the latter vs 106.6 kJ/mol in the former). Thus, it is difficult to unambiguously distinguish the solvent effect from the temperature dependence of the decomposition reaction.

Table 1 shows that the apparent activation energy for the decomposition reaction follows roughly a decreasing sequence as the reaction rate coefficient increases. The energy barrier for xanthates and dithiocarbonates are generally higher than those of trithiocarbonates and dithioesters. Striking deviations are nonetheless observed. For example, cumyl dithiobenzoate (**1**) shows unusually large E_{act}, which could be a consequence of the reverse coupling reaction. Trithiocarbonate **9** shows lower E_{act} than dithioesters **5** because the former decomposes through two pathways, as mentioned above. PMMA-RAFT (**16**) has E_{act} larger than expected, possibly due to difficulty in rotation of the C−S bond bearing a polymer chain. These side reactions and factors definitely cause complexity in the macroscopic reaction behavior of the thermal decomposition.

It is interesting to find from Figure 8c that the thermal stability of the universal RAFT agent strongly depends on its resting state, e.g., the neutral or protonated form. The neutral form, **17**, is very stable with E_{act} = 154.7 kJ/mol and $k_{dec,\ 333}$= 4.36 × 10^{-13} s^{-1}, the second highest stability of all RAFT/MADIX agents inspected. The protonated form, **18**, shows much higher tendency to decompose into a number of products. The products of the latter have not been isolated due to the low-resolution between peaks in HPLC (Supporting Information). Also, the reaction may have been complicated by the presence of *p*-toluenesulfonic acid. In Figure 9, the ^{1}H NMR spectrum of the reaction mixture after heating for 6 h in DMSO-d_6 shows remarkable weakening and diversifying of aromatic proton signals, possibly due to the coexistence of canonical structures of (4-pyridinyl)amine substituent. There is no or negligible signal assignable to vinyl protons of methyl acrylate, the expected product of β-elimination. The decomposition rate is 10^4 times faster than that of the neutral form (Table 1). This indicate that the universal RAFT agent does show two state of activities, which can be switched by protonation and deprotonation. The reason for larger activity in protonated form is due to strong electron withdrawing effect of quaternary ammonium ion.[75] The switch between two states renders the RAFT agent fascinating property to mediate the polymerizations of monomers with very different reactivity, such as MMA and vinyl acetate.[75]

CONCLUSION

Both the rate and mechanism of thermal decomposition closely relate to molecular structure of RAFT/MADIX agents. For thiocarbonylthio compounds possessing β-hydrogen, the primary pathway is Chugaev-type elimination. For those possessing α- but not β-hydrogen, the decomposition involves a phenylmethine carbene intermediate, resulting in the formation of (*E*)-stilbene. The universal RAFT agents shows a somewhat unexpected homolytic process, generating a thiocarbamoyl and an alkylthio radical, which undergoes rearrangement and coupling to form a new thiocarbamoyl species. In addition, thermal decomposition of xanthate on *O*- and *S*-sides seems to compete with each other.

The kinetic results demonstrate that the thermal stability of RAFT/MADIX agents is influenced concurrently by the structure of Z- and R-groups and closely relates to the decomposition pathway. For those undergo β-elimination, a remarkable difference in stability is observed among classes of thiocarbonylthio compounds with various Z-groups. Namely, dithioesters are much less stable than trithiocarbonates, xanthates, and dithiocarbamate. Here the stabilizing effect of lone pair donating Z-group, such as alkylthio (in trithiocarbonate), alkyloxy (in xanthates), and alkylamine (in dithiocarbamate), consorts with that observed in chain transfer reactivity. Within each class, those with more β-hydrogens and larger leaving groups give faster decomposition rate due to easier formation of the coplanar intermediate for concerted elimination. For those possessing only α-hydrogen, xanthates may be more active due to elimination from the *O*-alkyl side, while dithiocarbamates show highest stability without any hint of decomposition.

The destabilizing effect by the electron withdrawing Z-group is clearly illustrated by different stabilities of dithioesters in which Z = phenyl and nitrophenyl and by the universal RAFT agent at neutral and protonated state. This again consorts with the observation of activating effect of electron withdrawing groups on chain transfer reactivity of RAFT/MADIX agents.

The present work not only provides fundamental knowledge on thermal decomposition mechanism and kinetics, which is important for the removal of thiocarbonylthio termini of the RAFT/MADIX polymerizations products for the purpose of stabilization, but also sets the temperature limit of applicability of specific thiocarbonylthio compounds in RAFT polymerizations of different monomers. While most RAFT agents are stable at normal RAFT polymerization temperatures such as 60 °C, there are exceptions. For example, that cyanoisopropyl dithiobenzoate (**6**) decomposes at the rate coefficient of 2.57×10^{-6} s^{-1} at 60 °C (calculated), which is comparable to the rate of radical generation of AIBN (8.45×10^{-6} s^{-1}). If the conversion of **6** into corresponding polymeric dithioester is slow, the decomposition will cause retardation through radical quenching by the resulting dithiobenzoic acid. Thus, the data of stability of thiocarbonylthio compounds are very useful in optimizing the reaction conditions for the RAFT/MADIX polymerizations.

■ ASSOCIATED CONTENT

Supporting Information. HPLC, GC-MS, ^{1}H NMR, GPC, FT-IR, and UV−vis of concerned products and monitoring thermal decomposition reactions of certain thiocarbonylthio compounds. This material is available free of charge via the Internet at http://pubs.acs.org.

■ AUTHOR INFORMATION

Corresponding Author
*Phone: +86-21-65643509. E-mail: jphe@fudan.edu.cn.

■ ACKNOWLEDGMENT

This work is subsidized by the National Science Foundation of China (21174030). The authors thank Professor Ewald Daltrozzo for many helpful discussions.

■ REFERENCES

(1) Chiefari, J. C.; Chong, Y. K.; Ercole, F.; Krstina, J.; Jeffery, J.; Le, T. P. T.; Mayadunne, R. T. A.; Meijs, G. F.; Moad, C. L.; Moad, G.; Rizzardo, E.; Thang, S. H. *Macromolecules* **1998**, *31*, 5559–5562.
(2) Moad, G.; Rizzardo, E.; Thang, S. H. *Polymer* **2008**, *49*, 1079–1131.
(3) Moad, G.; Rizzardo, E.; Thang, S. H. *Acc. Chem. Res.* **2008**, *41*, 1133–1142.
(4) Boyer, C.; Bulmus, V.; Davis, T. P.; Ladmiral, V.; Liu, J.; Perrier, S. *Chem. Rev.* **2009**, *109*, 5402–5436.
(5) Moad, G.; Rizzardo, E.; Thang, S. H. *Aust. J. Chem.* **2005**, *58*, 379–410.
(6) Moad, G.; Rizzardo, E.; Thang, S. H. *Aust. J. Chem.* **2006**, *59*, 669–692.
(7) Favier, A.; Charreyre, M. *Macromol. Rapid Commun.* **2006**, *27*, 653–692.
(8) Corpart, P. C.; Charmot, D.; Biadatti, T.; Zard, S. Z.; Michelet, D. PCT Int. Appl. WO9858974,1998.
(9) Taton, D.; Wilczewska, A.-Z.; Destarac, M. *Macromol. Rapid Commun.* **2001**, *22*, 1497–1503.
(10) Destarac, M.; Bzducha, W.; Taton, D.; Gauthier-Gillaizeau, I.; Zard, S. Z. *Macromol. Rapid Commun.* **2002**, *23*, 1049–1054.
(11) Crotez-Lemus, N. A.; Salgado-Rodriguez, R.; Licea-Claverie, A. *J. Polym. Sci., Part A: Polym. Chem.* **2010**, *48*, 3033–3051.
(12) Menteiro, M. J.; Lonsdale, D. E. *J. Polym. Sci., Part A: Polym. Chem.* **2010**, *48*, 4496–4503.
(13) D'Agosto, F.; Hughes, R.; Charreyre, M.-T.; Pichot, C.; Gilbert, R. G. *Macromolecules* **2003**, *36*, 621–629.
(14) Pound, G.; McLeary, J. B.; McKenzie, J. M.; Lange, R. F. M.; Klumperman, B. *Macromolecules* **2006**, *39*, 7796–7797.
(15) Pound, G.; Aguesse, F.; McLeary, J. B.; Lange, R. F. M.; Klumperman, B. *Macromolecules* **2007**, *40*, 8861–8871.
(16) Vana, P.; Albertin, L.; Barner, L.; Davis, T. P.; Barner-Kowollik, C. *J. Polym. Sci., Part A: Polym. Chem.* **2002**, *40*, 4032–4037.
(17) Toy, A. A.; Vana, P.; Davis, T. P.; Barner-Kowollik, C. *Macromolecules* **2004**, *37*, 744–751.
(18) Favier, A.; Ladaviere, C.; Marie-Therese, C.; Pichot, C. *Macromolecules* **2004**, *37*, 2026–2034.
(19) Feldermann, A.; Toy, A. A.; Davis, T. P.; Stenzel, M. H.; Barner-Kowollik, C. *Polymer* **2005**, *46*, 8448–8457.
(20) Hart-Smith, G.; Lovestead, T. M.; Davis, T. P.; Stenzel, M. H.; Barner-Kowollik, C. *Biomacromolecules* **2007**, *8*, 2404–2415.
(21) Lovestead, T. M.; Hart-Smith, G.; Davis, T. P.; Stenzel, M. H.; Barner-Kowollik, C. *Macromolecules* **2007**, *40*, 4142–4153.
(22) Hart-Smith, G.; Chaffey-Millar, H.; Barner-Kowollik, C. *Macromolecules* **2008**, *41*, 3023–3041.
(23) Gruendling, T.; Hart-Smith, G.; Davis, T. P.; Stenzel, M. H.; Barner-Kowollik, C. *Macromolecules* **2008**, *41*, 1966–1971.
(24) Ladaviere, C.; Lacroix-Desmaze, P.; Delolme, F. *Macromolecules* **2009**, *42*, 70–84.
(25) Fandrich, N.; Falkenhagen, J.; Weidner, S. M.; Pfeifer, D.; Staal, B.; Thunemann, A. F.; Laschewsky, A. *Macromol. Chem. Phys.* **2010**, *211*, 869–878.
(26) Mayadunne, R. T. A.; Rizzardo, E.; Chiefari, J.; Krstina, J.; Moad, G.; Postma, A.; Thang, S. H. *Macromolecules* **2000**, *33*, 243–245.
(27) Wang, Z.; He, J.; Tao, Y.; Liu, Y.; Jiang, H.; Yang, Y. *Macromolecules* **2003**, *36*, 7446–7452.
(28) Patton, D. L.; Mullings, M.; Fulghum, T.; Advincula, R. C. *Macromolecules* **2005**, *38*, 8597–8602.
(29) Lima, V.; Jiang, X.; Brokken-Zijp, J.; Schoenmakers, P. J.; Klumperman, B.; Vanderlinde, R. *J. Polym. Sci., Part A: Polym. Chem.* **2005**, *43*, 959–973.
(30) Plummer, R.; Hill, D. J. T.; Whittaker, A. K. *Macromolecules* **2006**, *39*, 8379–8388.
(31) Xu, J.; He, J.; Fan, D.; Wang, X.; Yang, Y. *Macromolecules* **2006**, *39*, 8616–8624.
(32) Boyer, C.; Granville, A.; Davis, T. P.; Bulmus, V. *J. Polym. Sci., Part A: Polym. Chem.* **2009**, *47*, 3773–3794.

(33) Boyer, C.; Liu, J.; Bulmus, V.; Davis, T. P. *Aust. J. Chem.* **2009**, *62*, 830–847.
(34) Moad, G.; Chong, Y. K.; Postma, A.; Rizzardo, E.; Thang, S. H. *Polymer* **2005**, *46*, 8458–8468.
(35) Koo, S. P. S.; Stamenovic, M. M.; Prasath, R. A.; Inglis, A. J.; Prez, E. D.; Barner-Kowollik, C.; Camp, W. V.; Junkers, T. *J. Polym. Sci., Part A: Polym. Chem.* **2010**, *48*, 1699–1713.
(36) Schilli, C.; Lanzendoerfer, M. G.; Mueller, A. H. E. *Macromolecules* **2002**, *35*, 6819–6827.
(37) Aqil, A.; Qiu, H.; Greisch, J. F.; Jerome, R.; Pauw, E. D.; Jerome, C. *Polymer* **2008**, *49*, 1145–1153.
(38) Sumerlin, B. S.; Lowe, A. B.; Stroud, P. A.; Zhang, P.; Urban, M. W.; McCormick, C. L. *Langmuir* **2003**, *19*, 5559–5562.
(39) Scales, C. W.; Convertine, A. J.; McCormick, C. L. *Biomacromolecules* **2006**, *7*, 1389–1392.
(40) Zelikin, A. N.; Such, G. K.; Postma, A.; Caruso, F. *Biomacromolecules* **2007**, *8*, 2950–2953.
(41) Inglis, A. J.; Sinnwell, S.; Davis, T. P.; Barner-Kowollik, C.; Stenzel, M. H. *Macromolecules* **2008**, *41*, 4120–4126.
(42) Inglis, A. J.; Sinnwell, S.; Martina, H.; Stenzel, M. H.; Barner-Kowollik, C. *Angew. Chem., Int. Ed.* **2009**, *48*, 2411–2414.
(43) Sinnwell, S.; Inglis, A. J.; Davis, T. P.; Stenzel, M. H.; Barner-Kowollik, C. *Chem. Commun.* **2008**, 2052–2054.
(44) Li, C.; He, J.; Zhou, Y.; Gu, Y.; Yang, Y. *J. Polym. Sci., Part A: Polym. Chem.* **2011**, *49*, 1351–1360.
(45) Dietrich, M.; Glassner, M.; Gruendling, T.; Schmid, C.; Falkenhagen, J.; Barner-Kowollik, C. *Polym. Chem.* **2010**, *1*, 634–644.
(46) Willcock, H.; O'Reilly, R. K. *Polym. Chem.* **2010**, *1*, 149–157.
(47) Harvison, M. A.; Peter, J. R.; Davis, T. P.; Lowe, A. B. *Aust. J. Chem.* **2011**, *64*, 992–1006.
(48) Moad, G.; Rizzardo, E.; Thang, S. H. *Polym. Int.* **2011**, *60*, 9–25.
(49) Perrier, S.; Takolpuckdee, P.; Mars, C. A. *Macromolecules* **2005**, *38*, 2033–2036.
(50) Chong, Y. K.; Moad, G.; Rizzardo, E.; Thang, S. H. *Macromolecules* **2007**, *40*, 4446–4455.
(51) Chen, M.; Moad, G.; Rizzardo, E. *J. Polym. Sci., Part A: Polym. Chem.* **2009**, *47*, 6704–6714.
(52) Postma, A.; Davis, T. P.; Moad, G.; O'Shea, M. S. *Macromolecules* **2005**, *38*, 5371–5374.
(53) Chong, B.; Moad, G.; Rizzardo, E.; Skidmore, M.; Thang, S. H. *Aust. J. Chem.* **2006**, *59*, 755–762.
(54) Postma, A.; Davis, T. P.; Li, G.; Moad, G.; O'Shea, M. S. *Macromolecules* **2006**, *39*, 5307–5318.
(55) Postma, A.; Davis, T. P.; Evans, R. A.; Li, G.; Moad, G.; O'Shea, M. S. *Macromolecules* **2006**, *39*, 5293–5306.
(56) Xu, J.; He, J.; Fan, D.; Tang, W.; Yang, Y. *Macromolecules* **2006**, *39*, 3753–3759.
(57) Nejad, E. H.; Castignolles, P.; Gilbert, R. G.; Guillaneuf, Y. *J. Polym. Sci., Part A: Polym. Chem.* **2008**, *46*, 2277–2289.
(58) Albertin, L.; Stenzel, M. H.; Barner-Kowollik, C.; Davis, T. P. *Polymer* **2006**, *47*, 1011–1019.
(59) Plummer, R.; Goh, Y.-K.; Whittaker, A. K.; Monteiro, M. J. *Macromolecules* **2005**, *38*, 5352–5355.
(60) Favier, A.; Barner-Kowollik, C.; Davis, T. P.; Stenzel, M. H. *Macromol. Chem. Phys.* **2004**, *205*, 925–936.
(61) Chugaev, L. *Ber. Dtsch. Chem. Ges.* **1899**, *32*, 3332.
(62) Oconnor, G. L.; Nace, H. R. *J. Am. Chem. Soc.* **1952**, *74*, 5454–5459.
(63) Alexander, E. R.; Mudrak, A. *J. Am. Chem. Soc.* **1950**, *72*, 3194–3198.
(64) Alexander, E. R.; Mudrak, A. *J. Am. Chem. Soc.* **1951**, *73*, 59–62.
(65) Ahmed, S.; Luke A. Baker, L. A.; Grainger, R. S.; Innocenti, P.; Quevedo, C. E. *J. Org. Chem.* **2008**, *73*, 8116–8119.
(66) Liu, Y.; He, J.; Xu, J.; Fan, D.; Tang, W.; Yang, Y. *Macromolecules* **2005**, *38*, 10332–10335.
(67) Legge, T. M.; Slark, A. T.; Perrier, S. *J. Polym. Sci., Part A: Polym. Chem.* **2006**, *44*, 6980–6987.
(68) Chong, Y. K.; Krstina, J.; Le, T. P. T.; Moad, G.; Postma, A.; Rizzardo, E.; Thang, S. H. *Macromolecules* **2003**, *36*, 2256–2272.
(69) Chiefari, J.; Krstina, J.; Le, T. P. T.; Moad, G.; Postma, A.; Rizzardo, E.; Thang, S. H. *Macromolecules* **2003**, *36*, 2273–2283.
(70) Coote, M. L.; Radom, L. *J. Am. Chem. Soc.* **2003**, *125*, 1490–1491.
(71) Coote, M. L. *Macromolecules* **2004**, *37*, 5023–5031.
(72) Coote, M. L.; Radom, L. *Macromolecules* **2004**, *37*, 590–596.
(73) Coote, M. L.; Henry, D. J. *Macromolecules* **2005**, *38*, 1415–1433.
(74) Coote, M. L. *J. Phys. Chem. A* **2005**, *109*, 1230–1239.
(75) (a) Benaglia, M.; Chiefari, J.; Chong, Y. K.; Moad, G.; Rizzardo, E.; Thang, S. H. *J. Am. Chem. Soc.* **2009**, *131*, 6914–6915. (b) Benaglia, M.; Chen, M.; Chong, Y. K.; Moad, G.; Rizzardo, E.; Thang, S. H. *Macromolecules* **2009**, *42*, 9384–9386. (c) Keddie, D. J.; Guerrero-Sanchez, C.; Moad, G.; Rizzardo, E.; Thang, S. H. *Macromolecules* **2011**, *44*, 6738–6745.
(76) Le, T. P. ; Moad, G.; Rizzardo, E.; Thang, S. H. PCT Int. Appl. WO 9801478.
(77) Quinn, J. F.; Rizzardo, E.; Davis, T. P. *Chem. Commun.* **2001**, 1044–1045.
(78) Thang, S. H.; Chong, Y. K.; Mayadunne, R. T. A.; Moad, G.; Rizzardo, E. *Tetrahedron Lett.* **1999**, *40*, 2435–2438.
(79) Ladaviere, C.; Doerr, N.; Claverie, J. *Macromolecules* **2001**, *34*, 5370–5372.
(80) Movassagh, B.; Soleiman-Beigi, M.; Nazari, M. *Chem. Lett.* **2008**, *37*, 22–23.
(81) Destarac, M.; Brochon, C.; Catala, J. M.; Wilczewska, A.; Zard, S. Z. *Macromol. Chem. Phys.* **2002**, *203*, 2281–2289.
(82) Ishizu, K.; Khan, R. A.; Ohta, Y.; Furo, M. *J. Polym. Sci., Part A: Polym. Chem.* **2004**, *42*, 76–82.
(83) Ohara, K.; Inokuma, Y.; Fujita, M. *Angew. Chem., Int. Ed.* **2010**, *49*, 5507–5509.
(84) Moore, J. A.; Isaacs, T. *Tetrahedron Lett.* **1973**, *14*, 5033–5036.
(85) Hatanaka, K.; Tanimoto, S.; Oida, T.; Okano, M. *Tetrahedron Lett.* **1981**, *22*, 5195–5196.
(86) Hatanaka, K.; Tanimoto, S. *Tetrahedron Lett.* **1982**, *23*, 425–426.
(87) Corey, E. J.; Winter, E. *J. Am. Chem. Soc.* **1963**, *85*, 2677–2678.
(88) Horton, D.; Tindall, C. G., Jr. *J. Org. Chem.* **1970**, *35*, 3558–3559.
(89) Son, S.; Dodabalapur, A.; Lovinger, A. J.; Galvin, M. E. *Science* **1995**, *269*, 376–378.
(90) Kesters, E.; Gillissen, S.; Motmans, F.; Lutsen, L.; Vanderzande, D. J. M. *Macromolecules* **2002**, *35*, 7902–7910.
(91) Banishoeib, F.; Fourier, S.; Cleij, T. J.; Lutsen, L.; Vanderzande, D. J. M. *Eur. Phys. J.: Appl. Phys.* **2007**, *37*, 237–240.
(92) Nguyen, L. H.; Cleij, T. J.; Lutsen, L.; Vanderzande, D. J. M. *Sol. Energy Mater. Sol. Cells* **2006**, *90*, 2815–2828.
(93) Dilien, H.; Vandenbergh, J.; Banishoeb, F.; Adriaensens, P.; Cleij, T. J.; Lutsen, L.; Vanderzande, D. J. M. *Macromolecules* **2011**, *44*, 711–718.
(94) Henckens, A.; Colladet, K.; Fourier, S.; Cleij, T. J.; Lutsen, L.; Gelan, J. *Macromolecules* **2005**, *38*, 19–26.
(95) Henckens, A.; Duyssens, I.; Lutsen, L.; Vanderzande, D. J. M.; Cleij, T. J. *Polymer* **2006**, *47*, 123–131.
(96) Palmaerts, A.; van Haren, M.; Lutsen, L.; Cleij, T. J.; Vanderzande, D. J. M. *Macromolecules* **2006**, *39*, 2438–2440.
(97) Voronkov, M. G.; Panova, G. M.; Timokhina, L. V.; Gromkova, R. A. *Russ. J. Gen. Chem.* **2004**, *74*, 1043–1045.
(98) DePuy, C. H.; King, R. W. *Chem. Rev.* **1960**, *60*, 431–457.
(99) Arita, T.; Buback, M.; Vana, P. *Macromolecules* **2005**, *38*, 7935–7943.